ARTICLE
Journal of Cellular Biochemistry 111:665–675 (2010)

Journal of Cellular Biochemistry

Sumoylation Modulates a Domain in CTCF That Activates Transcription and Decondenses Chromatin

Neal S. Kitchen and Christopher J. Schoenherr*

Department of Cell and Developmental Biology, University of Illinois at Urbana-Champaign, Urbana, Illinois 61801

ABSTRACT

CTCF is a multipurpose transcription factor with activation, repression, and insulator activity. It also participates in regulating chromatin architecture by maintaining open chromatin and mediating long-range chromosomal interactions. Participation by CTCF in such diverse processes suggests that it has multiple functional domains that regulate transcription and modify chromatin structure. Using transient and integrated reporters, we identified a 107-amino-acid domain in CTCF's N-terminal region that is capable of transcriptional activation and chromatin decondensation. This domain demonstrated moderate transactivation when targeted to a promoter proximal position but showed little activity from more distal positions and on a natural promoter. By contrast, the activation domain dramatically decondensed the compact chromatin structure of a large transgene array, in a manner similar to the potent activation domain in VP16. In addition, the activation domain is subject to conjugation by SUMO, which reduced its transcriptional and chromatin opening activity. Moreover, mimicking full sumoylation by fusing Sumo-1 or -3 to the activation domain eliminated its transcriptional activity, but only Sumo-3 fusion prevented chromatin opening. We suggest that the activation domain's limited transactivation, but strong chromatin decondensation allows CTCF to establish and maintain open chromatin without necessarily activating transcription. Sumoylation may contribute to CTCF's enhancer blocking or repression functions by reducing transactivation and chromatin opening. J. Cell. Biochem. 111: 665–675, 2010.

KEY WORDS: CTCF; INSULATOR; CHROMATIN BOUNDARY; SUMO

CTCF is a zinc finger DNA binding protein that was first identified as a transcriptional repressor of the *c-myc* and chicken lysozyme genes [Baniahmad et al., 1990; Lobanenkov et al., 1990]. More recently, CTCF was shown to repress *hTERT* and *PAX6* [Li et al., 2004; Renaud et al., 2007]. On the other hand, CTCF activates *APP* and co-operates with CIITA and regulatory factor X to drive expression of two HLA genes [Vostrov and Quitschke, 1997; Majumder et al., 2008]. CTCF also co-operates with the thyroid hormone receptor to both positively and negatively regulate the transcription of several genes [Lutz et al., 2003]. CTCF, however, is best known as an insulator protein that blocks enhancer activity at *Igf2/H19*, chicken β-globin, and other loci [Phillips and Corces, 2009]. Insulators also prevent the spread of heterochromatin, and loss of CTCF binding correlates with the acquisition of repressive epigenetic marks and silencing of *c-myc*, *DM1*, and *p16(INK4a)* [Cho et al., 2005; Gombert and Krumm, 2009; Witcher and Emerson, 2009].

CTCF also regulates the architecture of the genome [Phillips and Corces, 2009]. Genome-wide analyses identified thousands of CTCF sites that are associated with nuclease sensitivity, increased histone methylation, and positioned nucleosomes, suggesting that CTCF directs localized remodeling of chromatin [Xi et al., 2007; Fu et al., 2008; Cuddapah et al., 2009]. Analyses of individual genes also showed open chromatin and higher levels of H3 and H4 acetylation surrounding CTCF sites [Litt et al., 2001; Han et al., 2008]. On a larger scale, results from chromosome conformation capture (3C) studies indicated that CTCF mediates interactions between distant intrachromosomal regulatory regions to form chromatin loops [Splinter et al., 2006; Xu et al., 2007; Yoon et al., 2007]. Similar results suggested that CTCF is required for interchromosomal interactions between *Xist* alleles in female cells and between the *Igf2/H19* and *Wsb1/Nf1* loci [Ling et al., 2006; Xu et al., 2007].

CTCF's diverse regulatory and structural functions are likely to require multiple functional domains throughout the protein. However, specific domains necessary for transactivation, enhancer blocking, or altering chromatin structure have not been identified. Limited functional mapping localized repression to the zinc finger and C-terminal regions, and both activation and repression

Additional Supporting Information may be found in the online version of this article.

Grant sponsor: NIH; Grant numbers: CA105017, GM007283.

*Correspondence to: Dr. Christopher J. Schoenherr, Department of Cell and Developmental Biology, University of Illinois at Urbana-Champaign, 601 S. Goodwin Ave., Urbana, IL 61801. E-mail: schoenhe@life.uiuc.edu

Received 9 March 2010; Accepted 11 June 2010 • DOI 10.1002/jcb.22751 • © 2010 Wiley-Liss, Inc.
Published online 29 June 2010 in Wiley Online Library (wileyonlinelibrary.com).

to its N-terminal region [Filippova et al., 1996; Burcin et al., 1997; Lutz et al., 2000; Vostrov et al., 2002]. In addition, a more extensive mapping identified a small repression motif in its N-terminal region [Drueppel et al., 2004]. In some cases, the transcriptional effects of CTCF and its domains varied substantially between cell types, suggesting additional levels of regulation [Lutz et al., 2000]. CTCF is also subject to modification by the small ubiquitin-like modifiers 1, 2, and 3 (SUMO) and to ADP-ribosylation, which contribute to its repression and enhancer blocking activity, respectively [Yu et al., 2004; MacPherson et al., 2009].

To better understand how CTCF performs its disparate functions, we mapped transcriptionally active portions of the protein and identified an activation domain (AD) in its N-terminal region that also alters chromatin structure. Detailed characterization of the domain indicated that it has moderate activity and limited ability to act over a distance. On the other hand, it induced large-scale chromatin decondensation of a lac operator array in a manner similar to the highly active VP16. Finally, we also showed that sumoylation of this domain suppressed its transactivation and chromatin opening activity.

MATERIALS AND METHODS

PLASMID CONSTRUCTS

The pLacR expression plasmid was constructed by modifying p3'SS-EGFP-dimer to include an SV40 NLS and a unique *Spe*I site at the C-terminus of the enhanced green fluorescent protein (EGFP) tagged-dimer *lac* repressor DNA-binding domain (DBD) [Tumbar et al., 1999]. To construct the empty expression vector, p3'SS, the GFP-LacR sequences were removed by digesting pLacR with *Xba*I and *Spe*I and religating. The pGal4 expression plasmid was constructed by modifying pcDNA3.1 to include three copies of the FLAG epitope, the SV40 NLS, and the Gal4 DBD followed by a unique *Xba*I site. Mammalian expression plasmids for hemagglutinin-tagged human Sumo-1, -2, and -3 and FLAG-tagged human SenP1 and mutant SenP1(C603S) were gifts of R.T. Hay.

The full-length murine CTCF cDNA was flanked with *Xba*I sites and inserted into the *Spe*I site of pLacR and the *Xba*I site of pGal4 to form pLacR-CTCF and pGal4-CTCF, respectively. All CTCF deletions were derived from PCR products amplified using primers ending in *Xba*I or *Spe*I sites. After digestion, the PCR products were inserted into pLacR and pGal4 to create in-frame fusions. The ADs of VP16 (amino acid residues 369–490), RelA (residues 286–519), and Sp1 (residues 100–313) were amplified and inserted into pLacR and pGal4 in a similar manner. Point mutations in CTCF fragments or Sumo-3 were generated by overlapping PCR. Sumo-1 and -3 cDNAs without the C-terminal glycine residues were amplified, digested with *Nhe*I and *Xba*I and ligated in frame with the NTAD (residues 44–150 of CTCF) in pLacR- and pGal4-NTAD. All PCR-derived constructs were sequenced to ensure fidelity. For the LacR constructs, protein expression was confirmed through Western blot analysis of whole-cell lysates using anti-GFP (Upstate Biotech, ms-1315) at 1:4,000. For the Gal4 constructs, anti-FLAG M2 (Stratagene) was used at 1:6,000. For expression in yeast, full-length CTCF, the NTAD, VP16 AD, and Sp1 AD were inserted into the *Nhe*I site of a modified pGBKT7 (Clontech).

The p5G-Luc reporter contains five Gal4 binding sequences adjacent to an E1b-TATA driven luciferase reporter. The p8L-Luc reporter contains eight lac operators adjacent to an E1b-TATA driven luciferase reporter (a gift from A. Belmont). To construct pH19-Luc, an *Eco*RV–*Sma*I fragment containing the murine H19 promoter (−250 to +17 bp) was inserted into *Sma*I-digested pGL3-Basic (Promega). To construct p5G-H19-Luc, five Gal4 UAS's were inserted into the *Nhe*I site of pH19-Luc, which is just upstream of the H19 promoter. In pH19-Luc-8L, eight lac operators were placed 2 kb downstream of luciferase by inserting a *Sal*I–*Xho*I fragment from p8L-Luc into the *Sal*I site of pH19-Luc. To construct p8L-Luc-5G, an *Xba*I–*Pst*I fragment containing the five Gal4 sites from p5G-Luc was inserted into p8L-Luc-NN digested with *Nhe*I–*Nsi*I. To construct p8L-Luc-NN, an *Nhe*I–*Nsi*I linker was inserted into the *Aat*II site of p8L-Luc, which is 3 kb downstream of luciferase.

TISSUE CULTURE, TRANSIENT TRANSFECTIONS, AND LUCIFERASE ASSAYS

Chinese hamster ovary cells (CHO) were cultured in F-12 Ham's medium with 10% fetal bovine serum (FBS) and COS7 and HeLa cells in DMEM 10% FBS. A03 cells were cultured in F-12 Ham's medium without hypoxanthine and thymidine, 10% dialyzed FBS, and 0.3 μM methotrexate. All cells were incubated at 37°C in 5% CO_2.

Transient transfections of A03 cells were performed on coverslips in 35 mm plates with 1 μg of the pLacR fusions and 4 μl of Mirus TransIT-LT1. Transient transfections of CHO, HeLa, and COS7 cells were performed in six-well plates for 48 h. Cells were harvested in lysis buffer (1% Triton, 50 mM Tris base, 25 mM phosphoric acid, 1 mM EDTA) and assayed in luciferase reaction buffer (400 mM Tris base, 200 mM phosphoric acid, 1 mg/ml BSA, 5 mM DTT, 0.3 mM D-luciferin, 3 mM ATP, 5 mM $MgCl_2$). Luciferase and β-galactosidase activity (CPRG) were measured using a Tecan ULTRA Evolution plate reader.

IMMUNOCYTOCHEMISTRY

Forty-eight hours after initiating transfection, coverslips containing A03 cells were rinsed twice in PBS-ME (Dulbecco's phosphate-buffered saline without Ca^{+2} and Mg^{+2}, 5 mM $MgCl_2$, 0.1 mM EDTA), permeabilized for 60 s in PBS-MET (PBS-ME, 0.1% Triton X-100), fixed in 1.8% formaldehyde in PBS-ME for 15 min at room temperature, and then quenched with three 5 min washes of PBS-ME with 20 mM glycine. The coverslips were then blocked at 4°C in PBS + 5% normal goat serum for 60 min, washed three times for 5 min each in PBS-MET and incubated at 4°C for 24 h with primary antibody diluted in PBS-MET at 1:500 for rabbit anti-acetylated tail H4 (Serotec AH418). After primary antibody incubation, coverslips were washed three times in PBS-MET and then incubated at 4°C overnight with Texas Red goat anti-rabbit IgG (Jackson ImmunoResearch) diluted 1:1,000 in PBS-MET. Coverslips were then washed three times with PBS-MET and stained with 0.2 μg/ml 4′,6-diamidino-2-phenylindole dihydrochloride (DAPI) for 5 min, followed by two PBS-ME rinses. Coverslips were mounted onto slides with a Mowiol-DABCO antifade reagent. For determining co-localization at the HSR, coverslips from at least three separate transfections were stained and 40 nuclei showing co-expression were scored.

IMAGING AND IMAGE ANALYSIS

Light microscopy images were taken in the DAPI, fluorescein, and Texas red channels on an inverted light microscope equipped with a cooled, slow-scan charge-coupled device camera (IMT-2; Olympus or Applied Precision OMX V2 with DeltaVision). Raw images were deconvolved as described [Robinett et al., 1996] or with softWoRx Suite (Applied Precision). Representative optical sections were processed using ImageJ. For quantifying HSR areas, a computer-controlled microscopy system collected images of the nuclei of transfected A03 cells in both the fluorescein and DAPI channels, as described [Carpenter et al., 2004]. The program only collected images of GFP fluorescence that was associated with a DAPI-stained nucleus and was above a minimum intensity to exclude cells expressing low levels of the GFP-LacR fusions. After image collection, cells with a high level of GFP fluorescence throughout the nucleus were manually excluded, as this condition prevented accurate localization of the targeted HSR. The program then determined the number of pixels within the nucleus that were above a threshold of GFP signal. For each fusion, the area of the HSR was determined in 50–150 nuclei in each of two independent transfections. To calculate the *P*-values, Student's *t*-tests with unequal variance and a set to 0.025 were performed using Microsoft Excel's Analysis ToolPak.

RESULTS

THE N-TERMINAL REGION OF CTCF ACTIVATES TRANSCRIPTION

CTCF has been reported to both activate and repress transcription in transient transfection assays [Ohlsson et al., 2001]. To determine its transcriptional activity in our hands, we constructed plasmids expressing full-length murine CTCF fused to the DBD of a GFP-tagged Lac repressor (LacR) or a Flag-tagged Gal4. Separate reporter plasmids consisted of eight sites for LacR or five for Gal4 just upstream of a minimal TATA box driving a luciferase gene. Using both LacR and Gal4 DBDs reduced the chance that our results would be specific to either fusion partner or reporter plasmid. As the array-bearing cells (A03) described below were derived from CHO cells, our initial co-transfections were performed in CHO, and we found that both CTCF fusions activated their appropriate luciferase reporters in these cells (Fig. 1A). Since transactivation conflicted with previous reports of repression by CTCF, we transfected Cos7 and HeLa cells to determine if this result was specific to CHO. However, among the three cell lines, we found that LacR-CTCF's activation ranged from 6- to 75-fold compared to LacR alone and from 1.2- to 14-fold by Gal4-CTCF. Of the two fusions, LacR-CTCF was consistently more active than Gal4-CTCF, and both were most active in CHO cells and least active in HeLa cells. Thus, our results from the three cell lines suggest that activation, but not repression, of reporter plasmids by CTCF is relatively common.

CTCF consists of a zinc finger DBD (ZF) that is flanked by N-terminal (NT) and C-terminal (CT) regions, and we determined which of the three were responsible for transactivation. Using both LacR and Gal4 fusions, transfection assays showed that much or all of CTCF's transactivation resides in the NT (Fig. 1A). In CHO cells, LacR-NT activated the luciferase reporter 21-fold over LacR alone, which was lower than the full-length CTCF fusion's 75-fold induction (Fig. 1A). By contrast, the Gal4-NT fusion was at least 10-fold more active than Gal4-CTCF in two cell lines. The activity differences between CTCF and its NT could reflect protein interactions specific to the full-length protein. In contrast to the NT, both DBD fusions to the CT region generally were inactive, although LacR-CT activated the reporter 2.6-fold in CHO cells. For the ZF domain, the LacR fusion showed no significant activation or repression, but Gal4-ZF produced three- to fivefold repression (Fig. 1A). For the NT, CT, and ZF fusions, Western analysis revealed similar levels of expression, and immuno-staining showed all fusions localized to the nucleus (Fig. 1B,C and data not shown). Ours results suggested that only the NT region of CTCF activates substantially and that significant differences in fusion activity can occur depending on DBD partners and cell types.

CTCF'S ACTIVATION DOMAIN IS COMPOSED OF PARTIALLY REDUNDANT SUBDOMAINS AND AN INHIBITORY SEQUENCE

To map CTCF's transactivation domain in more detail, we assayed a deletion series of the NT region (amino acids 1–270) fused to LacR and Gal4 (Fig. 2A). Although activation levels in the three cell lines and with both DBDs showed quantitative differences, overall results were qualitatively consistent. The one exception was the N(183–270) segment, for which the LacR fusion was relatively neutral,

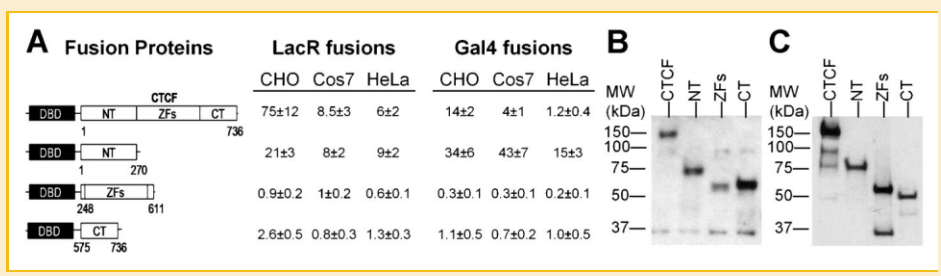

Fig. 1. The N-terminal region of CTCF activates transcription. A: Relative luciferase expression from CHO, Cos7, and HeLa cells transfected with the p8L-Luc reporter and LacR fusion plasmids or the p5G-Luc reporter and Gal4 fusion plasmids. The illustrations indicate the LacR or Gal4 fusion partners (DBD) and CTCF's N-terminal region (NT, residues 1–270), the zinc-finger DBD (ZFs, residues 248–611), and the C-terminal region (CT, residues 575–736). The amino acid residues are indicated below each construct. Normalized luciferase expression is relative to the control pLacR or pGal4 plasmids, taken as 1. The mean and standard deviation (SD) were derived from at least three independent experiments. Western analysis showing normalized protein expression of the LacR (B) and Gal4 (C) fusions after transfection in CHO cells. Similar results were seen in HeLa and Cos7 cells.

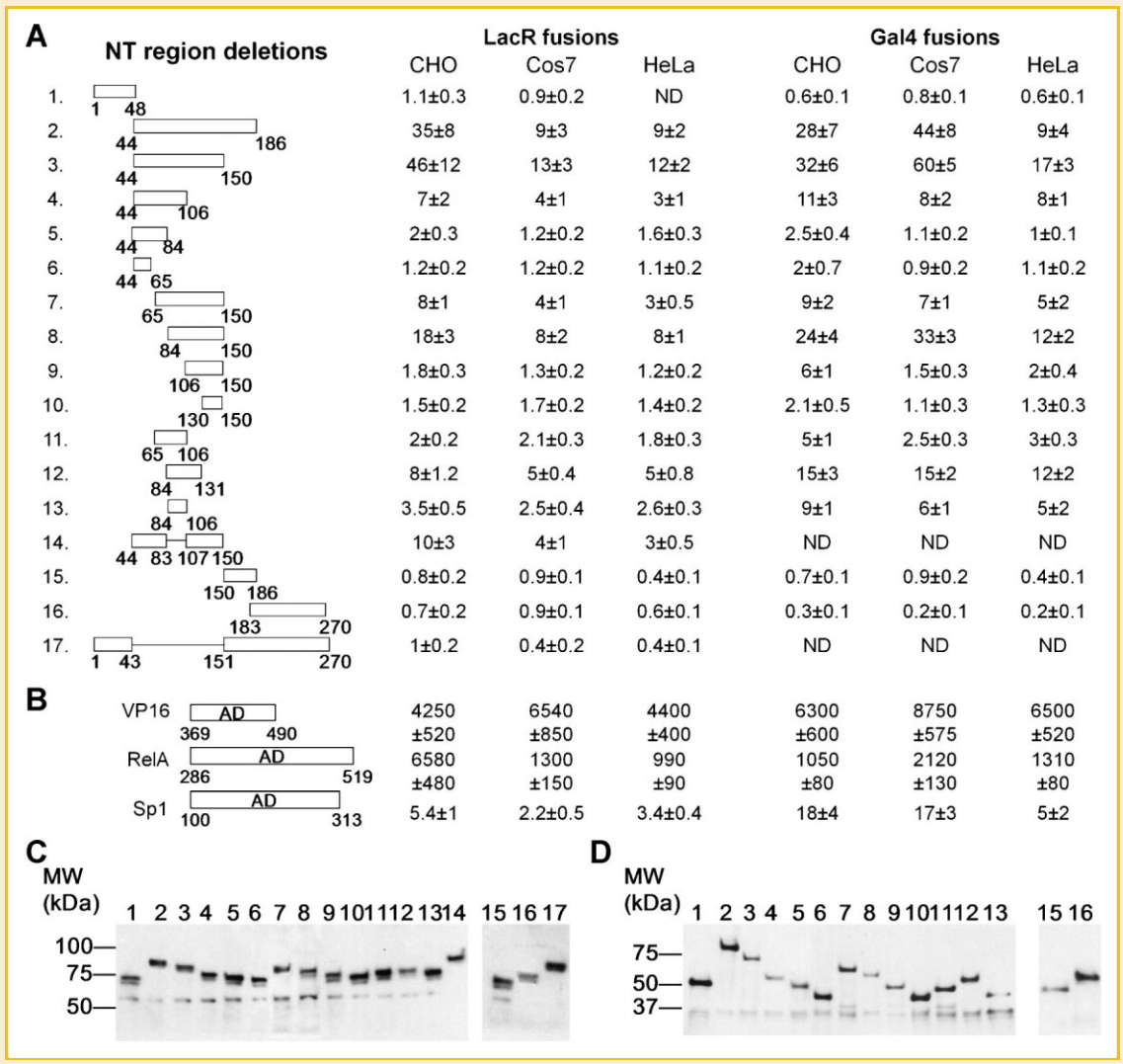

Fig. 2. CTCF's activation domain comprises three subdomains and one inhibitory sequence. A,B: Relative luciferase expression from CHO, Cos7, and HeLa cells transfected with the p8L-Luc reporter and LacR fusion plasmids or the p5G-Luc reporter and Gal4 fusion plasmids. The schematic illustrates the portions of the NT and the VP16, RelA, and Sp1 activation domains (AD) fused to the LacR and Gal4 DBDs. The amino acid residues are indicated below each construct. Normalized luciferase expression is relative to the control pLacR or pGal4 plasmids, taken as 1. The mean and SD were derived from at least three independent experiments. Luciferase activity of Gal4-VP16AD was not normalized to β-galactosidase expression due to apparent squelching of pSV-βgal. ND, not determined. Western blot analysis showing the normalized protein expression of the LacR (C) and Gal4 (D) NT fusions after transfection in CHO cells. Similar results were seen in HeLa and Cos7 cells. The numbers refer to the constructs shown in A.

while the Gal4 fusion repressed transcription three- to fivefold (Fig. 2A).

Our initial deletions indicated that most or all of the transactivation activity localized to N(44–150), and we mapped this further with a series of N- and C-terminal deletions (Fig. 2A). For the C-terminal deletions, the largest effect came from removing N(107–150). Further deletion of N(85–106) eliminated almost all transactivation, as the N(44–65) and N(44–84) fusions activated no more than 2.5-fold in any cell line. For the N-terminal deletions, removing N(44–64) caused a decrease in transactivation roughly equal to deleting N(107–150), which was unexpected as the N(44–65) segment by itself was almost inactive. Another surprise came from the N(84–150) fusion, which activated about two- to fivefold more than N(65–150) in all three cell lines. The increased activity suggested that N(65–83) contains an inhibitory motif and that activation by N(44–65) may balance the inhibition. As seen with the C-terminal deletion of this sequence, removing N(84–106) produced the largest percentage loss of activity, on average. Consistent with importance of this sequence, N(84–106) by itself averaged almost fivefold transactivation, and deleting it from N(44–150) reduced transactivation about fourfold. In contrast, N(44–65) and N(106–150) were important for the total activity of N(44–150), but both activated no more than twofold by themselves. Finally, deleting N(44–150) eliminated transactivation by the NT. Western blots showed similar expression levels of the deletions (Fig. 2B,C). All fusions had an SV40 NLS and were localized to the nucleus (data not shown). Thus, CTCF's AD, which we have termed the NTAD, maps to N(44–150) and consists of at least three partially redundant subdomains and a sequence that reduces its activity.

THE NTAD HAS TRANSCRIPTIONAL ACTIVITIES INTERMEDIATE TO ACIDIC AND GLUTAMINE-RICH ACTIVATION DOMAINS

To further characterize the NTAD functionally, we compared its activity in several assays to the acidic ADs from VP16 and p65 (RelA) and to the glutamine-rich AD from Sp1. In transfections of three cell lines using both Gal4 and LacR fusions, transcriptional activation by the VP16 and p65 ADs ranged from 1,000- to 9,000-fold when bound immediately adjacent to the minimal TATA box, while the Sp1 AD produced 2- to 18-fold activation (Fig. 2B). Thus, the 12- to 60-fold activation by the NTAD places it closer to the Sp1AD in promoter proximal activation. This pattern continued as Gal4-NTAD and -Sp1AD activated a minimal promoter less than threefold when using a reporter with the Gal4 UAS's positioned 3 kb from the TATA box (Fig. 3A). From this distal position, they also did not show synergistic activation when co-expressed with LacR-Sp1AD, which bound to promoter proximal sites (Fig. 3A). By contrast, the VP16 and p65 ADs activated about 18- to 70-fold and did synergize with LacR-Sp1AD (Fig. 3A). Similarly, LacR-NTAD and LacR-Sp1AD did not activate more than threefold when targeted immediately upstream of or 2 kb downstream of the H19 promoter (Fig. 3B,C), which has multiple Sp1 binding sites [Szabo et al., 1998].

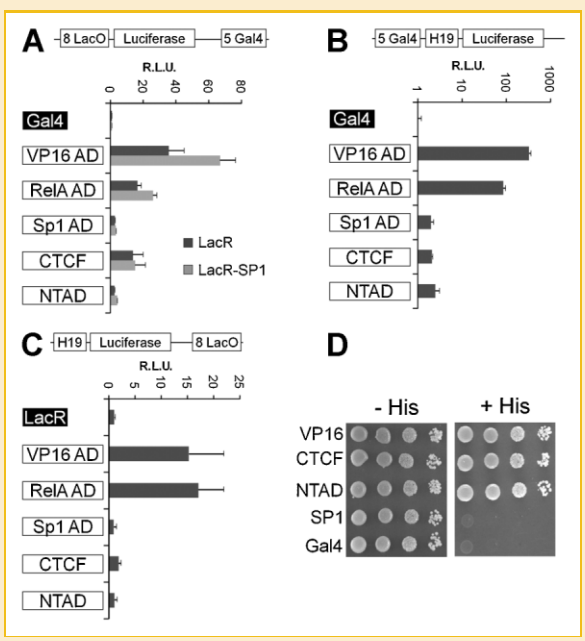

Fig. 3. Distal transactivation by the NTAD. A: Relative luciferase units (RLU) from CHO cells co-transfected with the indicated Gal4 fusion plasmids (0.5 μg), along with p8L-Luc-5G (diagram; 0.5 μg) and either pLacR (0.2 μg; dark gray) or pLacR-Sp1AD (0.2 μg; light gray). All transfections included pSV-βGal (0.1 μg). Normalized luciferase expression is relative to the control pLacR or pLacR-Sp1AD plasmids, taken as 1. Error bars indicate SD of at least three independent experiments. B: Logarithm of relative luciferase units from CHO cells co-transfected with p5G-H19-Luc (diagram; 0.5 μg) and Gal4 fusion plasmids (0.5 μg). C: Relative luciferase expression from CHO cells co-transfected with the pH19-Luc-8L reporter (diagram; 0.5 μg) and LacR fusion plasmids (0.5 μg). D: NTAD activates transcription of the Gal4-UAS driven *His3* in yeast. A fivefold dilution series of *S. cerevisiae* (strain AH109, Clontech) expressing the indicated Gal4 fusion proteins were spotted on to minimal media with and without histidine (His) and incubated for 3 days at 30°C.

Again, the VP16 and p65 ADs strongly activated the H19 promoter from both positions. Notably, in both distal reporter assays, the full-length CTCF fusions were more active than the NTAD, suggesting additional ADs in CTCF (Fig. 3B,C). In contrast to its activity in mammalian cells, the NTAD was more similar to acidic ADs in *Saccharomyces cerevisiae*, as Gal4 fusions to full-length CTCF, the NTAD, and the VP16 AD activated the His3 gene, whereas the Sp1 AD did not (Fig. 3D). Overall, the NTAD exhibited transactivation properties that were intermediate to those of acidic- and glutamine-rich ADs.

THE NTAD INDUCES HISTONE ACETYLATION AND DECONDENSES THE CHROMATIN STRUCTURE OF A TRANSGENE ARRAY

CTCF sites are frequently associated with open chromatin, histone acetylation, and phased nucleosomes [Fu et al., 2008], which suggest that CTCF elicits changes in chromatin and histone modifications. To provide direct evidence that CTCF can alter chromatin structure and to address whether the NTAD could contribute to that activity, we determined if the NTAD alters the structure of a large, stably integrated tandem array of a plasmid containing 256 *lac* operators (Fig. 4A). This array is present in the genome of a CHO cell derivative, A03, and appears as a condensed, heterochromatin-like structure that forms a 2 μm^2, DAPI-rich "homogeneously staining region" (HSR) (Fig. 4B) [Robinett et al., 1996]. Given its large size, decondensation or "opening" of the HSR can be visualized in the fluorescent microscope via GFP-tagged LacR fusions, and in that sense, the HSR is analogous to puffs formed by active genes in polytene chromosomes. Dramatic opening of the array, however, does not require transcription [Tumbar et al., 1999]. Moreover, previous studies and our results showed that only certain ADs were capable of decondensing the HSR [Carpenter et al., 2005]. For example, when bound by transiently expressed LacR-VP16AD or -p65AD, the condensed array often opened into numerous foci or fibrils that extended through much of the nucleus, which indicated substantial unfolding of the array's normally condensed chromatin (Fig. 4A,D,E) [Tumbar and Belmont, 2001]. On the other hand, arrays targeted by LacR fusions to the Sp1 AD or the proline-rich CTF AD never appeared larger than ones targeted by LacR alone (Fig. 4B and data not shown) [Carpenter et al., 2005]. By comparison, many of the arrays targeted by the LacR-NTAD resembled those bound by acidic ADs (Fig. 4F). Similar results were seen with LacR-CTCF fusions (data not shown). Finally, substantially opened arrays lost most or all of the enriched DAPI staining seen with the condensed array and were not generally associated with the DAPI-rich portions of the nucleus (Fig. S1).

Overall, the appearance of the HSRs targeted by LacR-NTAD varied from a single spot matching the condensed array to structures that spread through roughly a third of the nucleus. By eye, the degree of chromatin opening by NTAD appeared similar to that of the VP16 and p65 ADs, which was intriguing given that they were roughly 100-fold more active than the NTAD in the promoter proximal transactivation assays. In contrast, LacR-Sp1AD did not open the array, but activated only ninefold less than LacR-NTAD from the proximal position. To quantify the decondensation activity of the NTAD and VP16 AD, we measured the area that the targeted arrays encompassed using a computer-controlled microscope that

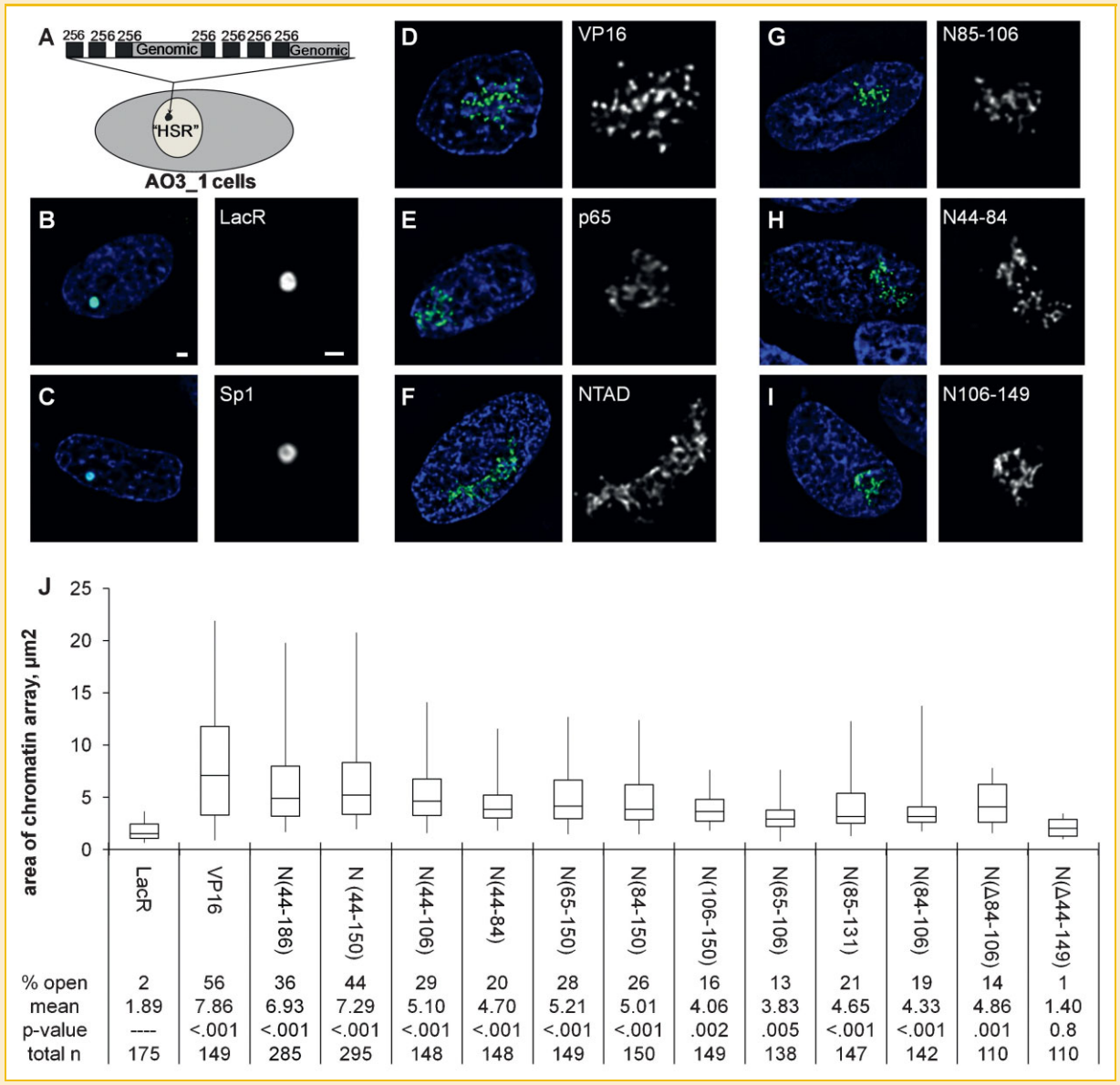

Fig. 4. The NTAD decondenses the chromatin structure of a lac operator transgene array. A: Illustration of the "homogeneously staining region" (HSR), a condensed chromatin structure comprising co-amplified concatamers of a vector with 256 direct lac operator repeats and hamster genomic DNA. B–I: Examples of "fully opened" arrays in A03 cells transfected with plasmids expressing the indicated LacR fusions. Images are deconvolved optical sections with the left panel showing DAPI (blue) merged with GFP signal (green). The right panel is an enlarged gray-scale image of the HSR. Scale bars, 1 μm. J: Box plots describing the range of HSR areas when targeted by LacR fusions. The end lines of the plot indicate the 10th and 90th percentiles; the box ends, the 25th and 75th percentiles; the centerline, the 50th percentile. The table below the box plots reports the % of "fully opened" arrays, the mean area of the HSRs (μm^2), the *P*-values for *t*-tests of the mean area compared to GFP-LacR alone, and the total number (n) of analyzed nuclei. Amino acid residues are indicated in parentheses. Arrays defined as "fully opened" had an area $>5.67\ \mu m^2$ (495 pixels), which is 3 standard deviations from the mean area of control GFP-LacR targeted HSRs ($1.89 \pm 1.26\ \mu m^2$).

collects digital images of nuclei with targeted arrays and determines the number of pixels within the nucleus that have GFP fluorescence above a minimum intensity [Carpenter et al., 2004]. After converting the pixel count into area, we defined as "fully opened" those arrays that encompassed an area greater than three standard deviations from the average size of control HSRs targeted by the inert LacR (Fig. 4J). In cells expressing LacR-NTAD, 44% of the targeted HSRs fulfilled this criterion, with an average area of 7.3 μm^2 (Fig. 4J). In the remainder of the expressing cells, 36% were "partially opened" (between 1 and 3 standard deviations greater than the control HSR), and 19% remained "condensed" (within 1 standard deviation). For comparison, the highly active LacR-VP16AD fully opened the HSR in 56% of expressing cells, with a mean area of 7.9 μm^2. To show that the NTAD's chromatin opening activity was not specific to A03 cells, we also transfected two additional CHO lines bearing similar *lac* operator arrays (D11, G12) [Tumbar et al., 1999] and found that the NTAD and VP16AD elicited similar levels of decondensation (data not shown). Finally, 85% (34/40 cells) of arrays bound by

LacR-NTAD showed high levels of staining for hyperacetylated histone H4, while staining was detectable in only 5% (2/40 cells) of LacR-bound arrays (Fig. 5). In comparison, strong staining was present at essentially 100% of arrays targeted by LacR-VP16AD (data not shown) [Tumbar et al., 1999]. Thus, in contrast to its modest transactivation, the NTAD demonstrated levels of array decondensation activity and H4 hyperacetylation that were similar to a strong acidic AD.

NTAD SUBDOMAINS CONTRIBUTE TO ITS CHROMATIN DECONDENSATION ACTIVITY

The contrast between the NTAD's modest transactivation and its strong chromatin opening activity suggested that they could be elicited by different portions of the NTAD and could reflect interactions with different transcriptional co-factors. Using the deletion series, we found that all of the NTAD segments tested were capable of inducing significant HSR decondensation, including ones that showed only twofold transactivation in the parent CHO cells (Fig. 4J). Moreover, each of the three main subdomains was capable of producing "fully opened" arrays, although at a much lower frequency (Fig. 4G–J). As seen with transactivation, quantifying the area encompassed by the targeted arrays showed that the NTAD deletions opened the HSR less than the full domain. In addition, the transcriptionally inactive N(1–48), N(183–270), N(149–186), and delta(N44–150) segments of the NT did not open the HSR (Fig. 4J and data not shown). As with transactivation, the entire NTAD contributes to chromatin decondensation (see Fig. S2 for a summary). However, the substantial opening activity of some subdomains with weak transactivation suggests distinct co-factor interaction.

SUMOYLATION MODULATES TRANSACTIVATION AND ARRAY DECONDENSATION BY THE NTAD

Our deletion analysis revealed an inhibitory segment within the NTAD that reduced its transactivation between two- and fivefold. We noted that this segment contains the sequence ^{72}MKTE, which matched the consensus for SUMO modification sites, ΨKXD/E, where Ψ is a bulky hydrophobic residue [Gill, 2005]. This motif is recognized by the SUMO E2, Ubc9, which ligates Sumo-1, -2, or -3 to the lysine residue in the SUMO modification sequence. After conjugation, SUMO-specific isopeptidases complete the cycle by removing SUMO from target proteins. Sumo-1 shares roughly 50% identity with Sumo-2 and -3, which are 95% identical and likely to be functionally equivalent. While this work was in progress, MacPherson et al. [2009] used biochemical techniques to show that lys73 was subject to sumoylation and found that sumoylation contributes to CTCF's repression of a reporter construct driven by the *c-myc* promoter . They did not, however, address how sumoylation affects transactivation and chromatin decondensation by CTCF's NTAD.

Many transcriptional activators are subject to conjugation by SUMO and, in most cases, the modification reduces their transactivation [Gill, 2005]. To test if the sumoylation motif inhibits NTAD activity, we created NTADR by changing lys73 to arginine, which prevents SUMO conjugation. We found that LacR-NTADR activated transcription from two- to threefold more than LacR-NTAD over a range of expression levels (Fig. 6A). In addition, co-expression of the SUMO isopeptidase, Senp1, increased activation by the NTAD but not the NTADR. A catalytically inactive Senp1 mutant had no effect on either fusion (Fig. 6B). Although it showed increased transactivation, the mean area of arrays targeted by LacR-NTADR was not significantly larger than those bound by LacR-NTAD in transfections of A03 cells (Fig. 6D). However, we confirmed that the NTAD fusion did recruit all three SUMO proteins to the HSR in a lys73-dependent manner (data not shown).

The moderate effect that sumoylation had on transactivation could indicate that a sumoylated NTAD is not strongly inhibited by the modification. However, for most target proteins, $<$10% of the total pool is sumoylated at any moment, which makes it difficult to

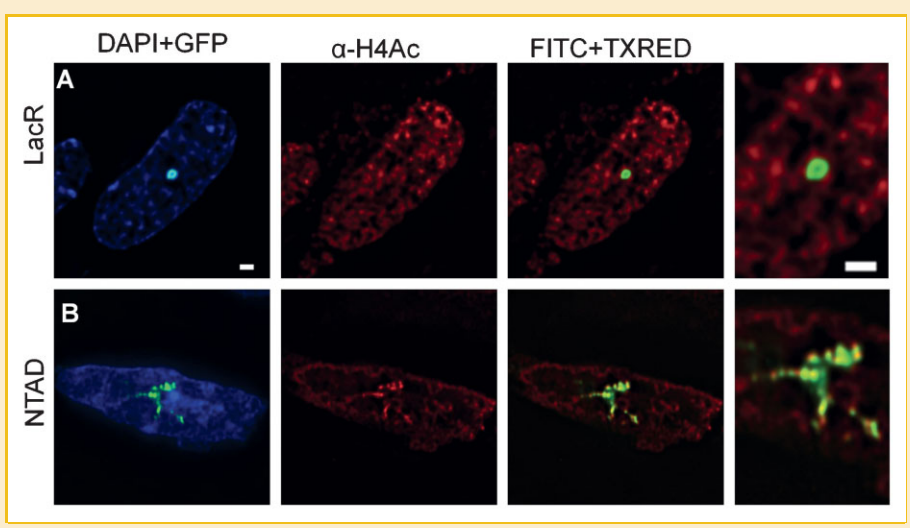

Fig. 5. The NTAD induces H4 hyperacetylation of a lac operator transgene array. Optical sections of nuclei from A03 cells transfected with pLacR (A) or pLacR-NTAD (B). The left panels show the GFP-tagged LacR or LacR-NTAD, the second show staining for hyperacetylated histone H4, the third show the merge. The last panel is an enlargement of the merge.

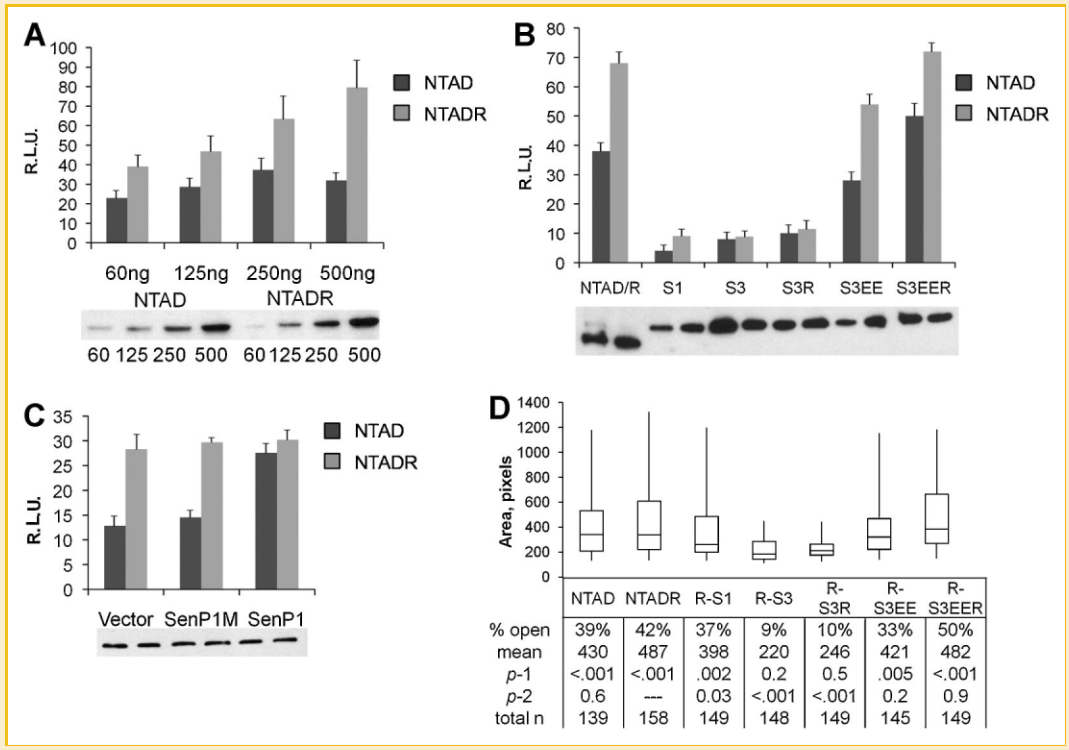

Fig. 6. Sumoylation modulates transactivation and array decondensation by the NTAD. A: Relative luciferase activity from CHO cells transfected with p8L-Luc (0.5 μg) and the indicated amounts of pLacR-NTAD (dark gray) or pLacR-NTADR (light gray). Empty expression plasmid (p3'SS) was added to bring total plasmid to 1.1 μg in each transfection. All transfections included pSV-βgal (0.1 μg). Error bars indicate SD of at least three independent experiments. B: Relative luciferase activity from CHO cells co-transfected with p5G-Luc (0.5 μg) and pGal-NTAD (0.2 μg; dark gray) or pGal-NTADR (0.2 μg; light gray) in the presence of 0.5 μg of pcDNA3 (Control), pcDNA3-SenP1(C603S) (SenP1M), or pcDNA3-SenP1 (SenP1). C: Relative luciferase expression in CHO cells co-transfected with p8L-Luc and plasmids expressing LacR-NTAD (0.5 μg; dark gray) or LacR-NTADR (0.5 μg; light gray) as translational fusions to conjugation-defective Sumo-1 (S1), Sumo-3 (S3), Sumo-3(D62R) (S3-U), Sumo-3(K32E, K41E) (S3-S), or Sumo-3(K32E, K41E, D62R) (S3-US). Western analysis with an antibody against GFP (A,C) or the Flag epitope (B) shows normalized protein expression levels. D: Box plots of HSR areas when targeted by NTAD or NTADR and its translational fusions to Sumo-1, Sumo-3, or Sumo-3 mutants. The table below the box plots reports the % of "fully opened" arrays, the mean area of the HSRs in pixels, the P-values for *t*-tests of the mean area compared to GFP-LacR alone (*p*-1) and LacR-NTADR (*p*-2), and the total number (n) of analyzed nuclei.

measure the activity of the sumoylated species [Hay, 2005]. To address this difficulty, we created translational fusions of the conjugation-defective Sumo-1 or -3 to the C-terminus of the LacR-NTAD and -NTADR to mimic full sumoylation [Ross et al., 2002]. In contrast to the twofold inhibition by the sumoylation motif, direct fusion of Sumo-1 and -3 led to nearly complete inhibition of both NTAD and NTADR transactivation (Fig. 6C). Notably, the NTAD-SUMO fusions were transcriptionally neutral, not repressive. In the decondensation assay, direct fusion of Sumo-3 almost completely suppressed the NTADR's opening activity to levels similar to the LacR control. Direct fusion of Sumo-1, however, reduced the NTADR's mean array area by only 18% (Fig. 6D).

Several co-repressors have SUMO interaction motifs (SIMs) and are recruited to conjugated proteins via a SIM interaction domain within the three SUMO proteins [Song et al., 2004; Ouyang et al., 2009]. To test the importance of this domain in our assays, we measured transactivation and array opening activity of the LacR-NTADR fused to a Sumo-3 with mutations (K32E, K41E) that prevent its interactions with co-repressors [Chupreta et al., 2005]. In both assays, the mutations nearly or completely eliminated Sumo-3's inhibitory activity, indicating that the SIM interaction domain was necessary for its inhibition of transactivation and chromatin opening (Fig. 6C,D). In contrast, a mutation (D62R) that reduces interaction with the Ubc9 [Knipscheer et al., 2007] had only a small effect on inhibition by Sumo-3. Combining the two, however, eliminated Sumo-3's inhibitory activity in both assays, suggesting that each surface contributes to repressing transactivation and decondensation.

DISCUSSION

CTCF is a multifunctional transcription factor that activates and represses transcription, as well as regulates chromatin architecture by mediating chromatin loop formation and positioning nucleosomes. It also functions as an insulator protein that blocks enhancer activity and maintains open chromatin [Ohlsson et al., 2001; Phillips and Corces, 2009]. To identify which portions of CTCF have the potential to participate in such divergent regulatory modes, we characterized a domain in CTCF's N-terminal region that activates transcription and alters chromatin structure. In addition, we found that sumoylation of this domain reduced its transactivation and chromatin opening activity.

CTCF is generally thought to regulate transcription by altering small- and large-scale chromatin architecture, and we initially attempted to delineate CTCF's transcriptional and chromatin modifying domains in a native chromatin context. However, as reported by others, we found that knockdown of CTCF inhibited cell growth and overexpression of CTCF either inhibited cell growth or could not be maintained (data not shown) [Rasko et al., 2001; Docquier et al., 2005]. Moreover, microarray analysis after CTCF knockdown showed gene expression changes of only two- to fourfold, which would greatly limit the range of measurable effects [Wendt et al., 2008]. Taken together, these difficulties prevented us from reliably replacing CTCF with deletion mutants and made analysis of its functional domains using endogenous genes technically impractical. Therefore, we chose to map functional domains using both transient reporter assays and the lac operator array. Transcriptional domains of many transcription factors have been determined using transfected reporters, and the lac operator array provides an assay for changes in native chromatin structure that is independent of transcription [Tumbar et al., 1999].

In transient assays, we showed that full-length CTCF generally activated transcription when fused to two different heterologous DBDs. Further analysis localized most or all transactivation to 107 amino acids in the center of the N-terminal region, while the CT and ZF regions showed minimal or no activation. The location of the NTAD is consistent with results that mapped transactivation to the NT using in vitro transcription in nuclear extracts [Vostrov et al., 2002]. On the other hand, several other studies showed that full-length CTCF and NT fusion proteins repressed transcription in transfection assays [Filippova et al., 1996; Lutz et al., 2000; Drueppel et al., 2004]. In contrast, we never saw repression by CTCF or its NT. Within the NT, however, the N(180–270) segment was repressive but only as a Gal4 fusion, not LacR. Similarly, the ZF region was a repressor only when fused to Gal4. Repression by these two domains agrees with results from Drueppel et al. [2004] and Lutz et al. [2000], respectively, but its dependence on the Gal4 DBD in our experiments makes definitive conclusions difficult. Previous studies also found strong repression mediated by the CT, whereas in our hands, it was either neutral or activated slightly [Filippova et al., 1996; Lutz et al., 2000]. The sources of these discrepancies are unknown, but our results suggest that the fusion partner and cell type have substantial influence on CTCF's activity in transfection assays.

More than 10,000 CTCF sites have been identified across the genome and, as expected for an insulator protein, about 55% are located in intergenic regions. However, about 10% are in promoters and 35% in genes [Cuddapah et al., 2009]. To better understand how CTCF might regulate transcription from different genomic positions, we further characterized the NTAD's transcriptional activities and compared them to ADs from enhancer and promoter factors. When targeted to promoter-proximal positions, the NTAD demonstrated moderate activity that was substantially less than that of the acidic VP16 and RelA ADs, but several fold more than the glutamine-rich Sp1 AD. Like the Sp1 AD, however, the NTAD demonstrated weak transactivation of a natural promoter and from a distance of 2–3 kb. The NTAD's intermediate activity suggests that in terms of transactivation it is distinct from both enhancer and promoter factors and that it directly contributes to gene activation only when bound to more promoter proximal positions.

Transcription factor ADs are often grouped into categories based on their amino acid composition [Triezenberg, 1995], and the ADs of a given category frequently share functional properties in different transcriptional assays [Triezenberg, 1995; Blau et al., 1996]. The NTAD is enriched in acidic and hydrophobic residues (19% DE; 33% ILMV), as well as the polar residues, glutamine/asparagine (14%). The abundance of acidic and hydrophobic residues resembles acidic ADs, although the NTAD is devoid of aromatic residues that acidic ADs often rely on for their potent transactivation [Triezenberg, 1995]. Similarly, the NTAD lacks glutamine clusters that characterize glutamine-rich ADs [Triezenberg, 1995]. Thus, as with its intermediate transcriptional activity, the NTAD's amino acid composition appears between both acidic and glutamine-rich ADs.

In contrast to its modest transcriptional activity, the average array decondensation by the NTAD was only about 13% less than the transcriptionally potent AD from VP16 (Fig. 4J) and greater than that of the p65 AD (N.S.K., unpublished work). In contrast, the Sp1 AD had no array opening activity. The NTAD and VP16 AD also elicited H4 hyperacetylation of the array to similar degrees. These results suggest that the NTAD has chromatin modifying activity comparable to strong transcriptional activators and are consistent with those showing that CTCF binding at many endogenous genes is associated with open chromatin and modified histones [Fu et al., 2008]. Therefore, we speculate that the NTAD participates in some of CTCF's architectural roles by recruiting chromatin opening and histone modifying proteins. Moreover, while it appears to maintain open chromatin, CTCF is not generally thought of as an activator [Phillips and Corces, 2009]. Thus, the NTAD's limited transactivation would allow CTCF to alter chromatin structure without necessarily activating transcription. Finally, the NTAD's properties of limited transactivation, strong chromatin opening, and induction of active histone marks fit well with some models in which insulator proteins are considered to be transcriptionally neutral and block heterochromatin by decondensing chromatin and/or modifying histones [Gaszner and Felsenfeld, 2006]. Other models for insulator activity stress the formation of isolated chromatin loops, and the NTAD's ability to open chromatin could facilitate interactions between distant insulators necessary for establishing these loops.

Several groups have shown that decondensation of the lac operator array in A03 cells does not require transcription [Tumbar et al., 1999; Ye et al., 2001; Carpenter et al., 2004]. This distinction creates the possibility that separable portions of the 107aa NTAD mediated its transactivation and array decondensation activity. Using deletion analysis, we found that most subdomains had both activities, but several of them demonstrated quantitative differences between their level of transactivation and HSR decondensation. For example, N(84–150) transactivated 10-fold more than N(106–150), but its average array area was only 25% higher. Conversely, some subdomains activated transcription no more than twofold, but often elicited substantial array decondensation. The general overlap of transactivation and HSR opening activity suggests that each subdomain contributes to both processes, while the quantitative differences in activity could reflect disparity in the strength of their interactions with certain co-factors.

Although consistent with CTCF's activation and barrier functions, the presence of an AD seemed counterintuitive in a protein that also has enhancer blocking and repression activities. However, some transcription factors are known to have positive and negative regulatory states and to switch between them upon post-translational modification. For example, the zinc finger protein, Sp3, becomes a repressor only when sumoylated [Stielow et al., 2008]. Similarly, CTCF was shown to be sumoylated on its N- and C-terminal regions, and the modification increased its repression of a *c-myc* reporter [MacPherson et al., 2009]. Our results, however, showed that the N-terminal SUMO modification site is within an AD, and the modification reduced but did not eliminate its transactivation. Moreover, while directly fusing SUMO to the NTAD nearly eliminated transactivation, it did not lead to transcriptional repression. We also found that full-length CTCF fused to SUMO did not repress transcription (data not shown). Thus, our results extend those of MacPherson et al. by putting sumoylation in the context of the NTAD and suggest that sumoylation suppresses its transactivation but does not necessarily convert CTCF into a repressor.

In addition to its transcriptional effects, we found that translational fusions of Sumo-3, but not Sumo-1, lead to a nearly complete loss of array decondensation by the NTAD. These results suggest that CTCF constitutively modified by Sumo-3 is unable to open chromatin and provide one of the few examples of activities that distinguish Sumo-3 from Sumo-1 [Ouyang et al., 2009]. Moreover, the prevention of array opening by Sumo-3 and its dependence on the SIM interaction domain is consistent with Sumo-3's exclusive interaction with the CoRest/LSD1/HDAC co-repressor complex [Ouyang et al., 2009]. Given SUMO's suppression of transactivation and chromatin opening, we speculate that CTCF molecules bound to sites requiring enhancer blocking or repressor activity are more often sumoylated than those requiring barrier or activator activity. Notably, $<10\%$ of CTCF is sumoylated [MacPherson et al., 2009], and it will be interesting to determine if this pool represents CTCF molecules bound to loci requiring its enhancer blocking or repression functions.

ACKNOWLEDGMENTS

We are grateful for helpful discussions and instruction from A. Belmont, S. Memedula, and other members of the Belmont Lab and for the generous use of their microscopy system. We are also thankful for the generous gifts of antibodies and plasmids from A. Belmont, B. Freeman, and R. Hay. We thank N. Shakoor, A. Gupta, S. Knutson, S. Jalli, and T. Mallidi for help with plasmid construction, and D. Zimmerman and P. Jones for discussions and critical reading of the manuscript. This work was supported by the National Institute of Health Grant RO1 CA105017 (C.J.S.) and the Cell and Molecular Biology Training Grant Program GM007283 (N.S.K.).

REFERENCES

Baniahmad A, Steiner C, Kohne AC, Renkawitz R. 1990. Modular structure of a chicken lysozyme silencer: Involvement of an unusual thyroid hormone receptor binding site. Cell 61:505–514.

Blau J, Xiao H, McCracken S, O'Hare P, Greenblatt J, Bentley D. 1996. Three functional classes of transcriptional activation domain. Mol Cell Biol 16: 2044–2055.

Burcin M, Arnold R, Lutz M, Kaiser B, Runge D, Lottspeich F, Filippova GN, Lobanenkov VV, Renkawitz R. 1997. Negative protein 1, which is required for function of the chicken lysozyme gene silencer in conjunction with hormone receptors, is identical to the multivalent zinc finger repressor CTCF. Mol Cell Biol 17:1281–1288.

Carpenter AE, Ashouri A, Belmont AS. 2004. Automated microscopy identifies estrogen receptor subdomains with large-scale chromatin structure unfolding activity. Cytometry A 58:157–166.

Carpenter AE, Memedula S, Plutz MJ, Belmont AS. 2005. Common effects of acidic activators on large-scale chromatin structure and transcription. Mol Cell Biol 25:958–968.

Cho DH, Thienes CP, Mahoney SE, Analau E, Filippova GN, Tapscott SJ. 2005. Antisense transcription and heterochromatin at the DM1 CTG repeats are constrained by CTCF. Mol Cell 20:483–489.

Chupreta S, Holmstrom S, Subramanian L, Iniguez-Lluhi JA. 2005. A small conserved surface in SUMO is the critical structural determinant of its transcriptional inhibitory properties. Mol Cell Biol 25:4272–4282.

Cuddapah S, Jothi R, Schones DE, Roh TY, Cui K, Zhao K. 2009. Global analysis of the insulator binding protein CTCF in chromatin barrier regions reveals demarcation of active and repressive domains. Genome Res 19: 24–32.

Docquier F, Farrar D, D'Arcy V, Chernukhin I, Robinson AF, Loukinov D, Vatolin S, Pack S, Mackay A, Harris RA, Dorricott H, O'Hare MJ, Lobanenkov V, Klenova E. 2005. Heightened expression of CTCF in breast cancer cells is associated with resistance to apoptosis. Cancer Res 65:5112–5122.

Drueppel L, Pfleiderer K, Schmidt A, Hillen W, Berens C. 2004. A short autonomous repression motif is located within the N-terminal domain of CTCF. FEBS Lett 572:154–158.

Filippova GN, Fagerlie S, Klenova EM, Myers C, Dehner Y, Goodwin G, Neiman PE, Collins SJ, Lobanenkov VV. 1996. An exceptionally conserved transcriptional repressor, CTCF, employs different combinations of zinc fingers to bind diverged promoter sequences of avian and mammalian c-myc oncogenes. Mol Cell Biol 16:2802–2813.

Fu Y, Sinha M, Peterson CL, Weng Z. 2008. The insulator binding protein CTCF positions 20 nucleosomes around its binding sites across the human genome. PLoS Genet 4:e1000138.

Gaszner M, Felsenfeld G. 2006. Insulators: Exploiting transcriptional and epigenetic mechanisms. Nat Rev Genet 7:703–713.

Gill G. 2005. Something about SUMO inhibits transcription. Curr Opin Genet Dev 15:536–541.

Gombert WM, Krumm A. 2009. Targeted deletion of multiple CTCF-binding elements in the human C-MYC gene reveals a requirement for CTCF in C-MYC expression. PLoS One 4:e6109.

Han L, Lee DH, Szabo PE. 2008. CTCF is the master organizer of domain-wide allele-specific chromatin at the H19/Igf2 imprinted region. Mol Cell Biol 28:1124–1135.

Hay RT. 2005. SUMO: A history of modification. Mol Cell 18:1–12.

Knipscheer P, van Dijk WJ, Olsen JV, Mann M, Sixma TK. 2007. Noncovalent interaction between Ubc9 and SUMO promotes SUMO chain formation. EMBO J 26:2797–2807.

Li T, Lu Z, Lu L. 2004. Regulation of eye development by transcription control of CCCTC binding factor (CTCF). J Biol Chem 279:27575–27583.

Ling JQ, Li T, Hu JF, Vu TH, Chen HL, Qiu XW, Cherry AM, Hoffman AR. 2006. CTCF mediates interchromosomal colocalization between Igf2/H19 and Wsb1/Nf1. Science 312:269–272.

Litt MD, Simpson M, Recillas-Targa F, Prioleau MN, Felsenfeld G. 2001. Transitions in histone acetylation reveal boundaries of three separately regulated neighboring loci. EMBO J 20:2224–2235.

Lobanenkov VV, Nicolas RH, Adler VV, Paterson H, Klenova EM, Polotskaja AV, Goodwin GH. 1990. A novel sequence-specific DNA binding protein which interacts with three regularly spaced direct repeats of the CCCTC-motif in the 5′-flanking sequence of the chicken c-myc gene. Oncogene 5:1743–1753.

Lutz M, Burke LJ, Barreto G, Goeman F, Greb H, Arnold R, Schultheiss H, Brehm A, Kouzarides T, Lobanenkov V, Renkawitz R. 2000. Transcriptional repression by the insulator protein CTCF involves histone deacetylases. Nucleic Acids Res 28:1707–1713.

Lutz M, Burke LJ, LeFevre P, Myers FA, Thorne AW, Crane-Robinson C, Bonifer C, Filippova GN, Lobanenkov V, Renkawitz R. 2003. Thyroid hormone-regulated enhancer blocking: Cooperation of CTCF and thyroid hormone receptor. EMBO J 22:1579–1587.

MacPherson MJ, Beatty LG, Zhou W, Du M, Sadowski PD. 2009. The CTCF insulator protein is posttranslationally modified by SUMO. Mol Cell Biol 29:714–725.

Majumder P, Gomez JA, Chadwick BP, Boss JM. 2008. The insulator factor CTCF controls MHC class II gene expression and is required for the formation of long-distance chromatin interactions. J Exp Med 205:785–798.

Ohlsson R, Renkawitz R, Lobanenkov V. 2001. CTCF is a uniquely versatile transcription regulator linked to epigenetics and disease. Trends Genet 17: 520–527.

Ouyang J, Shi Y, Valin A, Xuan Y, Gill G. 2009. Direct binding of CoREST1 to SUMO-2/3 contributes to gene-specific repression by the LSD1/CoREST1/HDAC complex. Mol Cell 34:145–154.

Phillips JE, Corces VG. 2009. CTCF: Master weaver of the genome. Cell 137:1194–1211.

Rasko JE, Klenova EM, Leon J, Filippova GN, Loukinov DI, Vatolin S, Robinson AF, Hu YJ, Ulmer J, Ward MD, Pugacheva EM, Neiman PE, Morse HC III, Collins SJ, Lobanenkov VV. 2001. Cell growth inhibition by the multifunctional multivalent zinc-finger factor CTCF. Cancer Res 61:6002–6007.

Renaud S, Loukinov D, Abdullaev Z, Guilleret I, Bosman FT, Lobanenkov V, Benhattar J. 2007. Dual role of DNA methylation inside and outside of CTCF-binding regions in the transcriptional regulation of the telomerase hTERT gene. Nucleic Acids Res 35:1245–1256.

Robinett CC, Straight A, Li G, Willhelm C, Sudlow G, Murray A, Belmont AS. 1996. In vivo localization of DNA sequences and visualization of large-scale chromatin organization using lac operator/repressor recognition. J Cell Biol 135:1685–1700.

Ross S, Best JL, Zon LI, Gill G. 2002. SUMO-1 modification represses Sp3 transcriptional activation and modulates its subnuclear localization. Mol Cell 10:831–842.

Song J, Durrin LK, Wilkinson TA, Krontiris TG, Chen Y. 2004. Identification of a SUMO-binding motif that recognizes SUMO-modified proteins. Proc Natl Acad Sci USA 101:14373–14378.

Splinter E, Heath H, Kooren J, Palstra RJ, Klous P, Grosveld F, Galjart N, de Laat W. 2006. CTCF mediates long-range chromatin looping and local histone modification in the beta-globin locus. Genes Dev 20:2349–2354.

Stielow B, Sapetschnig A, Wink C, Kruger I, Suske G. 2008. SUMO-modified Sp3 represses transcription by provoking local heterochromatic gene silencing. EMBO Rep 9:899–906.

Szabo PE, Pfeifer GP, Mann JR. 1998. Characterization of novel parent-specific epigenetic modifications upstream of the imprinted mouse H19 gene. Mol Cell Biol 18:6767–6776.

Triezenberg SJ. 1995. Structure and function of transcriptional activation domains. Curr Opin Genet Dev 5:190–196.

Tumbar T, Belmont AS. 2001. Interphase movements of a DNA chromosome region modulated by VP16 transcriptional activator. Nat Cell Biol 3:134–139.

Tumbar T, Sudlow G, Belmont AS. 1999. Large-scale chromatin unfolding and remodeling induced by VP16 acidic activation domain. J Cell Biol 145:1341–1354.

Vostrov AA, Quitschke WW. 1997. The zinc finger protein CTCF binds to the APBbeta domain of the amyloid beta-protein precursor promoter. Evidence for a role in transcriptional activation. J Biol Chem 272:33353–33359.

Vostrov AA, Taheny MJ, Quitschke WW. 2002. A region to the N-terminal side of the CTCF zinc finger domain is essential for activating transcription from the amyloid precursor protein promoter. J Biol Chem 277:1619–1627.

Wendt KS, Yoshida K, Itoh T, Bando M, Koch B, Schirghuber E, Tsutsumi S, Nagae G, Ishihara K, Mishiro T, Yahata K, Imamoto F, Aburatani H, Nakao M, Imamoto N, Maeshima K, Shirahige K, Peters JM. 2008. Cohesin mediates transcriptional insulation by CCCTC-binding factor. Nature 451:796–801.

Witcher M, Emerson BM. 2009. Epigenetic silencing of the p16(INK4a) tumor suppressor is associated with loss of CTCF binding and a chromatin boundary. Mol Cell 34:271–284.

Xi H, Shulha HP, Lin JM, Vales TR, Fu Y, Bodine DM, McKay RD, Chenoweth JG, Tesar PJ, Furey TS, Ren B, Weng Z, Crawford GE. 2007. Identification and characterization of cell type-specific and ubiquitous chromatin regulatory structures in the human genome. PLoS Genet 3:e136.

Xu N, Donohoe ME, Silva SS, Lee JT. 2007. Evidence that homologous X-chromosome pairing requires transcription and CTCF protein. Nat Genet 39: 1390–1396.

Ye Q, Hu YF, Zhong H, Nye AC, Belmont AS, Li R. 2001. BRCA1-induced large-scale chromatin unfolding and allele-specific effects of cancer-predisposing mutations. J Cell Biol 155:911–921.

Yoon YS, Jeong S, Rong Q, Park KY, Chung JH, Pfeifer K. 2007. Analysis of the H19ICR insulator. Mol Cell Biol 27:3499–3510.

Yu W, Ginjala V, Pant V, Chernukhin I, Whitehead J, Docquier F, Farrar D, Tavoosidana G, Mukhopadhyay R, Kanduri C, Oshimura M, Feinberg AP, Lobanenkov V, Klenova E, Ohlsson R. 2004. Poly(ADP-ribosyl)ation regulates CTCF-dependent chromatin insulation. Nat Genet 36:1105–1110.